

Preparation of Y-TZP ceramic fibers by electrolysis-sol-gel method

Jianjun Li · Xiuling Jiao · Dairong Chen

Received: 26 April 2006 / Accepted: 19 September 2006 / Published online: 4 April 2007
© Springer Science+Business Media, LLC 2007

Abstract Polycrystalline yttria stabilized tetragonal Zirconia (T-ZrO₂) fibers were obtained by pyrolysis of gel fibers using zirconium oxychloride octahydrate as raw material. The spinnable zirconia sol was prepared by electrolyzing the zirconium oxychloride octahydrate solution in the presence of acetic acid and sugar (sucrose, glucose or fructose), in which the molar ratio of CH₃COOH/ZrOCl₂ · 8H₂O and sugar/ZrOCl₂ · 8H₂O was in the range of 1.0–4.0 and 0.2–0.4, respectively. The relation of spinnability to the shape of colloidal particle was discussed. The as-prepared zirconia fibers sintered at different temperatures show smooth and crack-free surface with the diameter of 5–10 μm. Slow heating rate below 600 °C and then sintering at 1,400 °C for 30 min were necessary to obtain the dense tetragonal zirconia ceramic fibers, the particles composed the fibers had the size of ~150 nm.

Introduction

As a widely used ceramics fiber material, the continuous Zirconia (ZrO₂) fiber has attracted great interest for several decades as high strength reinforcement material with melting point of over 2,700 °C and excellent chemical resistance to reactive environments, etc [1]. In past decades, many routes to the ZrO₂ fibers have been developed. For example, cellulose fibers impregnated with zirconium

salts were sintered to remove the organic matrix to form the zirconia fibers [2], and zirconium alkoxide/salts hydrolyzed to form polyzirconoxane [3] or organozirconium complexes [4], which were converted to zirconia fibers. The sol-gel process containing the spinning of the sol from zirconium acetate [5], alkoxide [6, 7] or oxychloride [8, 9] to form the gel fibers and the sintering of gel fibers was a potential method.

Although the sol-gel method was extensively studied, many problems still remained. The greatest limitation to the synthesis of ceramics fibers by the sol-gel process was the expensive precursor, especially the alkoxide compound. The aqueous sol-gel technology was suitable for industrial production, but it was limited in preparing ceramics fibers. The electrolysis of inorganic zirconium salts had several advantages over the conventional sol-gel method [10], in which the expensive metal alkoxide or organometallic complexes could be effectively avoided, the hydrolysis and condensation could be controlled by changing the potential and/or current. Our group [11] reported the preparation of ZrO₂ fiber by use of the electrolysis combined with sol-gel method from ZrOCl₂ · 8H₂O solution using H₂SO₄ as complexant, however, in that process the quantity of H₂SO₄ must be controlled exactly to avoid coagulation or precipitate producing, and the presence of SO₄²⁻ might decrease the quality of the ceramic fiber due to its high decomposing temperature. Therefore it was necessary to develop a more facile and controllable synthetic route to ZrO₂ fiber with high quality.

In the present work, the crack-free yttria stabilized T-ZrO₂ (YSZ) fibers with smooth surface and the diameter of 5–10 μm were prepared by the electrolysis combined with the sol-gel method. The sugar was used to enhance the stability of sol, in which the carboxyl groups

J. Li · X. Jiao (✉) · D. Chen
Department of Chemistry, Shandong University, Jinan 250100,
P.R. China
e-mail: jjaoxl@sdu.edu.cn

coordinated to Zr(IV) yielded the zirconium acetate complex, favoring the formation of long linear polymer species and spinnable sol.

Experimental

Preparation

ZrOCl₂ · 8H₂O and Y(NO₃)₃ · 6H₂O (the molar ratio of Y₂O₃ to ZrO₂ was 0.025) were dissolved in distilled water, and the sucrose was added to form a transparent solution. The solution was then heated at 40 °C under magnetic stirring for 1 h, after one third of the needed acetic acid added, the solution was electrolyzed at 25 °C for 48–60 h to obtain the sol. To obtain the spinnable sol, the remained acetic acid was added into the sol after the solution was electrolyzed for ca. 10 h. From the experiment, the optimal molar ratios of CH₃COOH/ZrOCl₂ · 8H₂O and sugar/ZrOCl₂ · 8H₂O are respectively 2.0 and 0.2, and the concentration of ZrOCl₂ · 8H₂O is 3.1 mol/L. After the electrolysis process completing, the sol was first aged in air to present a thick film at the surface with the solvent vaporizing, and then aged for 5–8 days in a closed system to form the homogenous sol. A continuous green fiber could be drawn at 1.0 m/s speed by immersing a glass rod with a diameter of ca. 5 mm into the sol and pulling it up, and then dried at 70 °C for 24 h and sintered under air atmosphere in four stages: (1) from room temperature to 600 °C at a rate of 0.5 °C/min, (2) holding at 600 °C for 2 h, (3) raising to designed temperature at a rate of 10 °C/min, (4) holding at the temperature for 2 h. Finally the ZrO₂ fibers were obtained after cooling to room temperature naturally.

Characterization

X-ray diffraction (XRD) patterns of the prepared samples were recorded on an X-ray diffractometer (Rigaku D/Max 2200PC) with a graphite monochromator and CuK_α radiation ($\lambda = 0.15148$ nm) at room temperature while the voltage and electric current were held at 28 kV and 20 mA. Thermal gravimetric (TG) analysis (TGA/SDTA, 851° METTLER) at a rate of 50 mL/min in air flow and heating rate of 20 °C/min was employed to measure the weight loss of the xerogel fibers. The morphology and surface microstructure of the fibers were observed using a scanning electron microscopy (SEM, JEOL JXA-840). IR spectra of the fibers were measured on Fourier transform infrared spectrophotometer (Nicolet, 5DX FTIR) using KBr pellet technique after the fibers were ground into powders. The sol viscosity was analyzed on a cone-and-plate rheometer (RS75 (HAAKE)) at room temperature. The absorption spectra of solution and sol from 200 to 1,100 nm were

recorded on an UV–Vis spectrophotometer (Lambda 35, Perkin-Elmer). Nitrogen adsorption-desorption data were measured with an a Quantachrome QuadraSorb SI apparatus at liquid nitrogen temperature ($T = -196$ °C). Isotherms were evaluated with the Barrett–Joyner–Halenda (BJH) theory to give the surface areas and pore distribution. All specimens for characterization are prepared at the optimal preparation condition: CH₃COOH/ZrOCl₂ · 8H₂O is 2.0, sugar/ZrOCl₂ · 8H₂O is 0.2, [ZrOCl₂ · 8H₂O] is 3.1 mol/L, and current density is 450 A/m².

Results and discussion

Preparation of the spinnable sol

In the present experiment, the optimal electrolysis temperature is 25–35 °C and the suitable current density is 150–450 A/m². Though the reactions carried out during the electrolyzing process are complicated, the main electrode reactions occur as described in previous report [11], in which the Cl₂ and H₂ gases are released from positive and negative electrodes respectively. With the electrolysis proceeding, the solution gradually turns into the colorless sol. Further electrochemical reaction will cause the condensation of sol particles, and the linear polymers are formed in presence of acetic acid and sugar. With the electrolysis end-point approaching, the sol becomes viscous and its viscosity increases with aging. As shown in Fig. 1, the spinnable sol exhibits as Newtonian or near-Newtonian flow with the viscosity of ~10 mPa·s after the precursor solution was electrolyzed at 25 °C for 50 h and then aged at room temperature for 5 days. The transparent green fibers as long as 300 cm could be drawn directly from the spinnable sol.

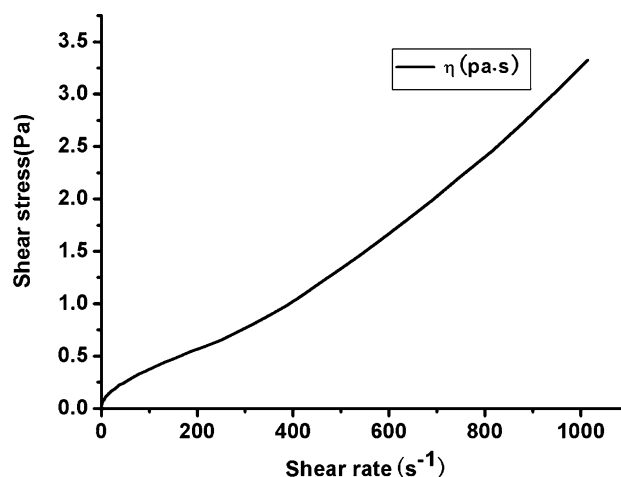


Fig. 1 Relation of the shear stress to the shear rate of the spinnable sol

Table 1 shows the effect of CH₃COOH on the spinnability of zirconium sol. When the molar ratio CH₃COOH to ZrOCl₂ · 8H₂O was larger than 1, the sol exhibited excellent spinnability, and the optimal ratio was 1.5–2.0. Further increasing the molar ratio to 4, the sol still possessed good spinnability, but the xerogel fibers became brittle due to the rapid vaporization of excessive acetic acid at the green fiber surface. At the same time, those listed in Table 2 shows that the spinnable sol could be obtained while the molar ratio of sugar to ZrOCl₂ · 8H₂O was 0.2–0.4 with a suitable ZrOCl₂ · 8H₂O concentration, and the optimal molar ratio of sugar to ZrOCl₂ · 8H₂O was 0.2. When the ratio was smaller than 0.1 or larger than 0.6, the white precipitate appeared during the electrolyzing process or sol showed no spinnability after electrolysis, respectively.

It was found that the absence of sugar resulted in the rapid gelation or precipitation during the electrolyzing process, and the sugar played an important role in holding sol stable during the hydrolysis and condensation. Chemical evolution of sugar (sucrose, glucose or fructose) was complicated in the present acidic solution, in which the sucrose molecules firstly hydrolyzed to form D-glucose and D-fructose [12], the fructose and glucose could form an enediol, which coordinated to the zirconyl cations. In order to understand the chemical evolution, the UV–Vis spectra were recorded after the solution was heated at 40 °C for 30 and 70 min and electrolyzed for 15 min, 11 and 24 h, respectively. Before analysis, the solutions were diluted until the ZrOCl₂ · 8H₂O concentration decreased to 0.005 mol/L. As shown in Fig. 2a, the absorptions at ca. 275 and 335 nm might be attributed to the zirconyl–sugar complex as shown in Fig. 3 [13]. The formation of the zirconyl–sugar complex prevented the precipitation or rapid gelation during electrolysis. However, the zirconyl–sugar complex was destructed progressively with the electrolyzing (Fig. 2b). After electrolyzed for ca. 10 h, the absorptions at ca. 275 and 335 nm almost disappeared and

the absorption band at ca. 218 nm might be due to the enediol from the decomposition of zirconium–sugar complex or monose acidification. The IR spectrum of the xerogel fibers (Fig. 5a) shows the C=C stretching vibration at 1,671 cm⁻¹, indicating the decomposition of the sugar–zirconium complex between the zirconium and oxygen. Here, the zirconium acetate was the principal zirconium complex species. As a complexing reagent, the CH₃COOH molecules could be used to adjust the spinnability of zirconium sol and prolong the gelation time by coordinating to Zr(IV) [14]. As known, the CH₃COOH molecules could coordinate to Zr(IV) by several modes including unidentate, bidentate chelating and bidentate bridging modes [15], which could be distinguished from the frequency separation between the asymmetric and symmetric carboxyl stretching vibrations of COO⁻. Figure 5b shows the asymmetric and symmetric vibrations of acetate at 1,561 and 1,384 cm⁻¹, and no absorptions of free acetic acid (1,720 and 1,295 cm⁻¹), indicating the acetic acid coordinating to Zr(IV). The frequency separation of 177 cm⁻¹ (between 1,561 and 1,384 cm⁻¹) suggests that the carboxyl group coordinated to zirconium by bidentate bridging mode [15]. The coordination of acetate to Zr(IV) is important in slowing the hydrolysis of Zr(IV) and assisting the complex condensation or polymerization to form the linear polymers for the preparation of the spinnable sol.

The particle shape can be deduced from the rheological properties of the sol [16]. If polymers in the solution are linear or chain-like, the reduced viscosity, η_{sp}/C of a polymer solution can be expressed by Huggin's Equation (1) [17].

$$\frac{\eta_{sp}}{C} = [\eta] + K[\eta]^2 C \quad (1)$$

where $\eta_{sp} = \eta_{rel} - 1$. $\eta_{rel} = \eta/\eta_0$, η -viscosity of solution; η_0 -viscosity of solvent. Here, η_{sp} , η_{rel} , K_C and C are the specific viscosity, the relative viscosity, the proportionality constant and the concentration of the polymer, respectively. The definition of limiting viscosity number $[\eta]$ is

$$[\eta] = \lim_{C \rightarrow 0} \frac{\eta_{rel} - 1}{C} = \lim_{C \rightarrow 0} \frac{\eta_{sp}}{C}$$

$[\eta]$ can be determined by extrapolation of the η_{sp}/C versus C relation to zero concentration of the polymer. The reduced viscosity η_{sp}/C of the solution containing spherical particles can be expressed by the Eq. (3) [18].

$$\frac{\eta_{sp}}{C} = \frac{K_C}{\rho}$$

K_C is a constant, ρ is the density of colloidal particles and C is the concentration of the polymer.

Table 1 Effects of CH₃COOH on the spinnability of zirconium sol^a

sol	CH ₃ COOH/ZrOCl ₂ · 8H ₂ O (molar ratio)	Gelation time (days)	Spinnability (cm)
1	0	1	No
2	0.3	1.5	No
3	0.5	5	No
4	1.0	7	100
5	1.5	4	200
6	2.0	7	300
7	4.0	6	200

^a The ZrOCl₂ · 8H₂O concentration was held at 3.1 mol/L, sugar/ZrOCl₂ · 8H₂O = 0.2

Table 2 Gelling characteristics of precursor solutions of various compositions^a

sol	ZrOCl ₂ · 8H ₂ O (wt%)	Sugar/ZrOCl ₂ ·8H ₂ O (molar ratio)	Gelation time (days)	Spinnability (cm)
1	30	0.2	15	100
2	30	0.4	1	No
3	30	0.6	1.5	No
4	50	0.1	12	No
5	50	0.2	7	300
6	50	0.4	8	50
7	70	0.2	7	100
8	70	0.4	7	50

^a The molar ratio of CH₃COOH to ZrOCl₂ · 8H₂O was 2.0

Fig. 2 UV spectra of zirconyl–sugar complexes after reacted at 40 °C for 30 and 70 min (a), or electrolyzed for 15 min., 11 and 24 h, respectively (b)

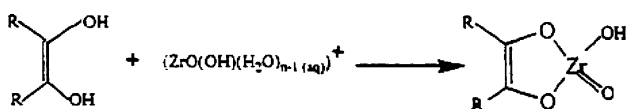
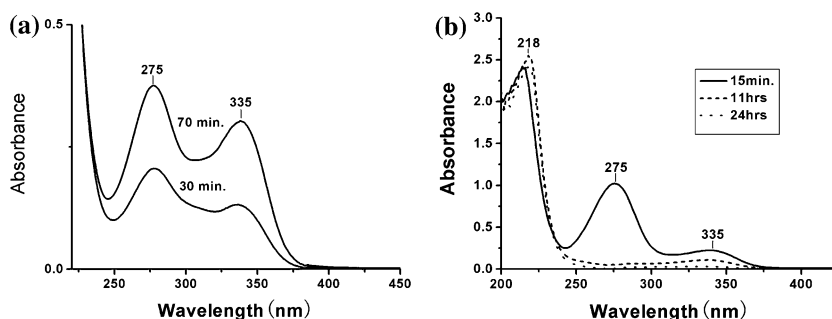


Fig. 3 The proposed reaction mechanism of zirconyl–sugar complex

The rheological property of the zirconium sol in Fig. 1 indicated that the sol was Newtonian or near-Newtonian fluid. After the spinnable sol diluted to 0.2, 0.3 and 0.4 mol/L (Zr(IV) concentration), the measured η_{sp}/C values were in agreement with Eqs. (1) and (2). The plot of reduced viscosity versus concentration (Fig. 4) indicated that the η_{sp}/C value increased with the concentration, indicating that particles maintained the linear shape [19].

Evolution of gel fibers

Figure 5 shows the IR spectra of the xerogel fibers and those sintered at different temperatures. The assignment of the absorptions in Fig. 4b is listed in Table 3. The sharp peak at 2,336 cm⁻¹ corresponding to CO₂ appears, indicating the absorption of CO₂ on the fibers. Upon calcined at 200 °C, the IR spectrum shows no obvious change except the decreasing of the absorption at 1,629 cm⁻¹, although there is ca. 20% weight loss before 200 °C from the TG curve (Fig. 6), indicating that the mass loss of ca. 20% below 220 °C is attributed to the evaporation of the absorbed water and a few of free acetic acid. The shoulder at

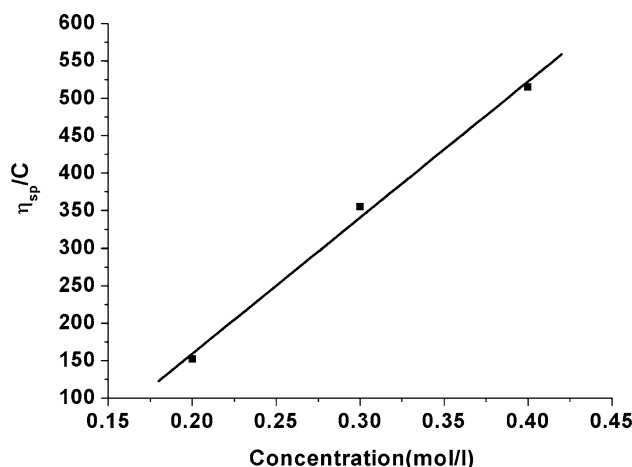


Fig. 4 Relation of viscosity of the sol to its concentration

1,671 cm⁻¹ is attributed to the C=C stretching vibration, indicating that the enediol is produced from the decomposition of zirconium–sugar complex, which disappears after sintered at 390 °C. The frequencies of the sugar derivative (1,403, 1,453 and 1,350 cm⁻¹ of CH₂ bending vibration and the coupling vibrations of OCH, CCH, and COH) in gel fibers shift to lower values in comparison to the corresponding vibrations (1,428, 1,456, and 1,360 cm⁻¹) in free sugar, indicating different status of the sugar derivatives upon coordination to zirconium [20, 21]. After sintering at 390 °C, the bands disappear, suggesting that

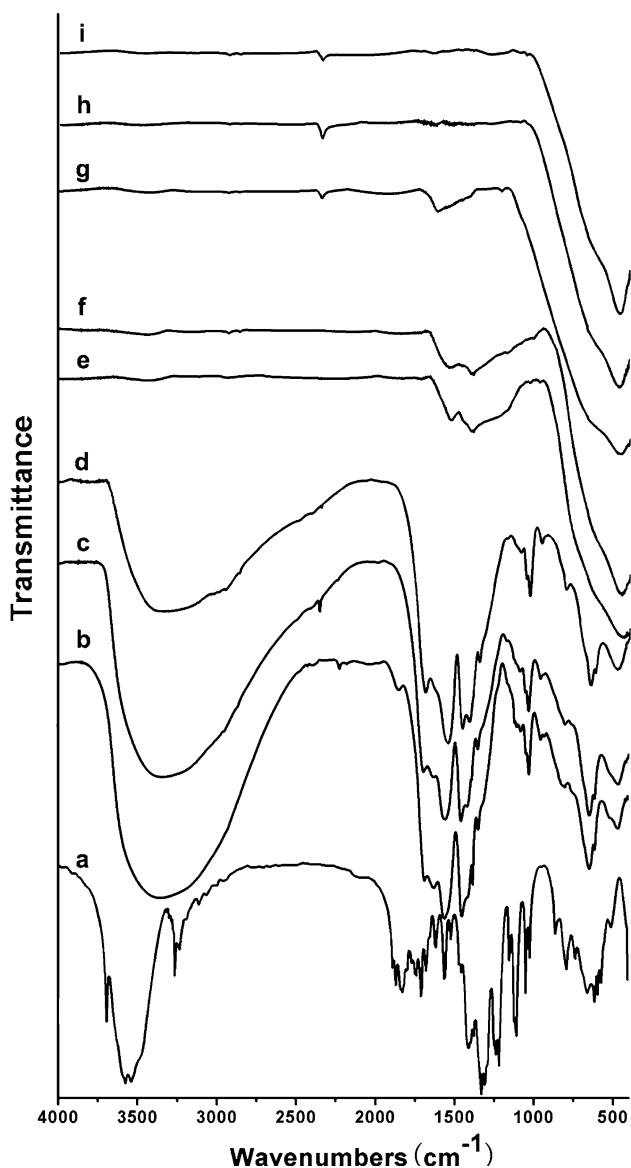


Fig. 5 IR spectra of sugar (a), gel fibers (b) and sintered fibers at 100 °C (c), 200 °C (d), 390 °C (e), 440 °C (f), 550 °C (g), 600 °C (h), and 800 °C (i)

the sugar derivatives are decomposed at that temperature. The sharp bands at 1,565 and 1,384 cm^{-1} attributed to the asymmetric and symmetric vibrations of the bridge coordinated COO^- almost disappear at 600 °C, indicating that zirconium acetate is decomposed, which is in agreement with the thermal analysis. The TG and DTG curves shown in Fig. 6 demonstrates the marked mass loss of 22% below 220 °C and the mass loss of 6.7% from 220 to 600 °C is due to the decomposition of most zirconium acetate and sugar derivatives. The bands at 1,085, 1,028 and 956 cm^{-1} (Fig. 5b) indicate the presence of double bonded zirconyl group Zr=O in the gel fibers [22–24]. The absorptions at 650 and 469 cm^{-1} are assigned to the deformation mode of

Table 3 The assignment of IR spectra of xerogel fibers

Wavenumber (cm^{-1})	Assignment
3400	O-H stretching vibration in carboxylate and water
2336	O=C=O (adsorbed CO_2)
1671	C=C stretching vibrations
1629	H-O-H bending vibration of H_2O
1561, 1384	asymmetric and symmetric vibrations of the bridge coordinated COO^-
1409	CH_2 bending vibration
1453, 1350	the coupling vibrations of OCH, CCH and COH
1085, 1028, 956	Zr=O vibration
650	deformation mode of the acetate groups
469	Zr-O-Zr vibration

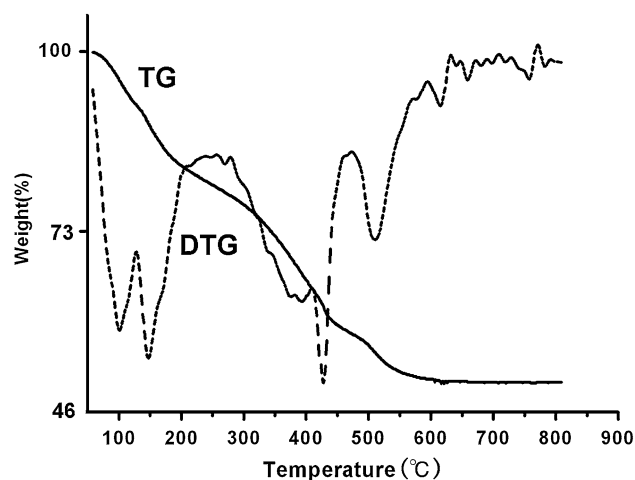


Fig. 6 TG and DTG curves of the xerogel fiber

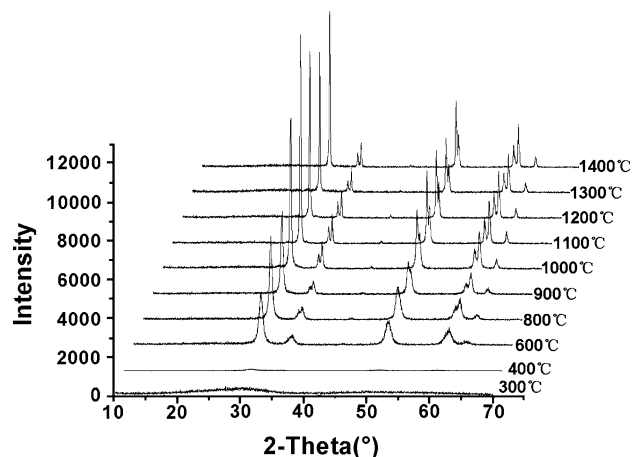
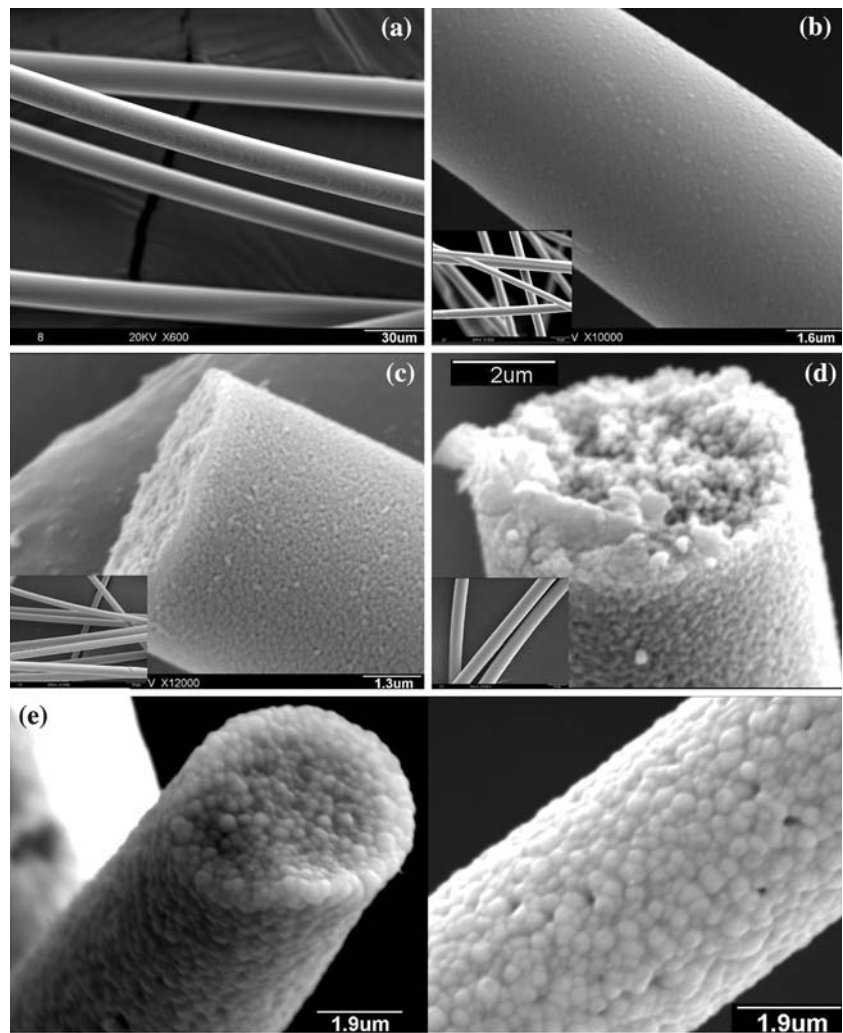


Fig. 7 XRD patterns of the products sintered at different temperatures

Fig. 8 SEM images of xerogel fibers (a) and those sintered at different temperatures: 900 °C (b), 1,100 °C (c), 1,200 °C (d), and 1,400 °C (e)



the acetate groups and Zr–O–Zr vibration, respectively, and those of the acetate groups disappear after heating at 390 °C. The intensity of Zr–O–Zr vibration increases with the calcination temperature rising, and the band at 740 cm^{-1} does not appear, indicating that no monoclinic ZrO₂ forms in the final fibers.

The XRD patterns (Fig. 7) reveal the T-ZrO₂ nature of the fibers, which begins to form at 400 °C (JCPDS file: No.48-0224). With the calcined temperature increasing, the peaks change sharper with the increased intensity, showing the increasing of the crystallinity and grain size of T-ZrO₂, which is in well agreement with the SEM images.

Microstructure evolution of the sintered fibers

Figure 8 shows SEM images of the xerogel fibers and those calcined at 900–1,400 °C. The xerogel fibers have the diameter of ca. 15–18 μm, while the diameter of calcined fibers decreases to ca. 5–10 μm due to the shrinkage caused by heat treatment. Both of the xerogel fibers and those

calcined ones exhibit uniform diameter without marked defects. The fibers have smooth and dense surface, and the grain size and pores significantly increase with the temperature raising. The individual nano-scale grains are apparent (Fig. 8c) and the grain size significantly increases from 900 to 1,100 °C, but there is a slower grain growth between 1,100 and 1,200 °C. At 1,400 °C, the grains change much coarser and microscopic pores are observed on the fiber's surface. There is a rapid increasing of the grain size at this temperature, and at this stage, dense ZrO₂ ceramics fibers are formed.

As known, the removing of the volatile substances from the solidified gel fibers at high temperature might produce some defects such as pores, cracks and bubbles, which decrease the fiber strength. In the as-prepared ZrO₂ fibers, the cracks can be effectively avoided, and the compact fibers are formed upon calcination. Zarzycki [25] and Scherer [26] have investigated the relationship between the stresses produced during drying and the capillary pores in a gel. They revealed that the larger pores decrease the cap-

Fig. 9 Pore size distribution of zirconia fibers sample 1 and sample 2 (in Table 4), first dried at 70 °C in air and vacuum (0.1 MPa) for 24 h, respectively, then heated in air up to 600 °C at the rate of 0.5 °C/min for 2 h

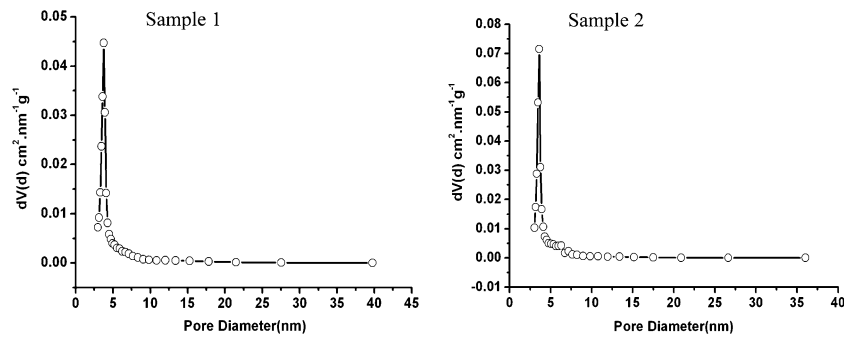


Fig. 10 Microstructure of sintered zirconia fibers at 1,300 °C for 10 min (a) and 30 min (b), at 1,400 °C for 10 min (c) and 30 min (d), at 1,500 °C for 5 min (e), and 15 min (f), respectively

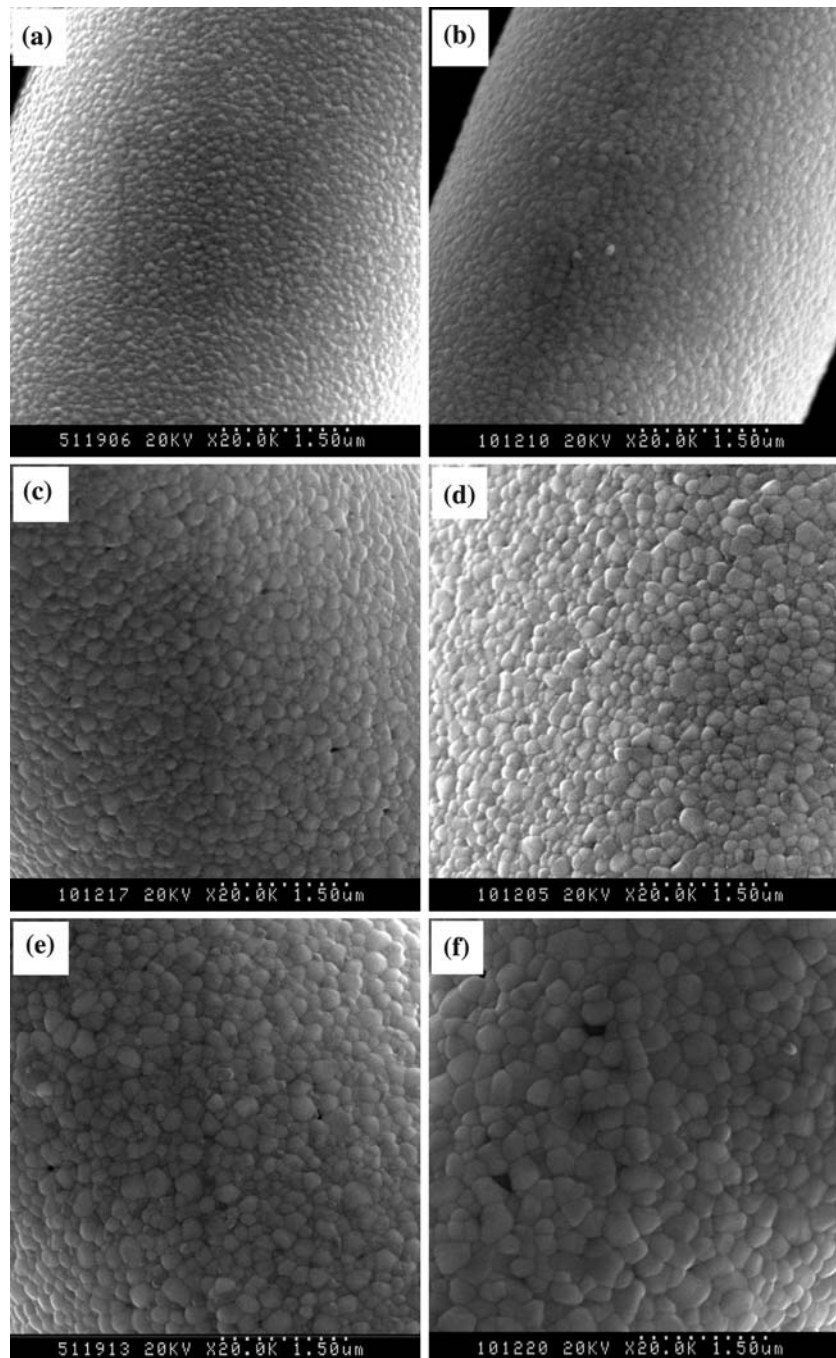


Table 4 Surface areas of sintered fibers at different temperatures

Sample	Sintering temp. (°C)	Surface area (m ² /g)
1	600	52.7
2 ^a	600	41.7
3	800	51.7
4	1,100	2.1
5	1,200	0.97
6	1,300	0.16
7	1,400	–
8	1,500	–

^a The sample was first dried at 70 °C in vacuum (0.1 MPa, the others dried in air) for 24 h and then heated in air up to the designed temperature according to Sect. “Preparation” mentioned

illary stresses and make it easier to synthesize the unfractured fibers. To decrease the capillary stresses, the comparative study of the gel fibers drying in air and vacuum is showed in Fig. 9 and Table 4, the green fibers were first dried at 70 °C in air (sample 1) and vacuum (0.1 MPa, sample 2) for 24 h, respectively, then sintered under air atmosphere up to 600 °C at the rate of 0.5 °C/min for 2 h. The pore size distribution of sample 1 and 2 showing that the mean pore diameters are both close to ca. 3.6 nm (Fig. 9), and the surface areas are 52.7 and 41.7 m²/g, respectively. It can be seen that the green fibers drying in air and vacuum conditions at 70 °C have a little difference and slow heating rate before removing the volatile substances is important and efficient for densification. Table 4 obviously shows that the surface area of the fibers significantly decreases with the temperature increasing, and the sample calcined at 1,300 °C shows a high density.

As densification proceeding, the pores slowly disappear and the drag forces exerted on the grain boundary gradually decrease, and some grains grow fast. So heating the fibers rapidly to a high temperature and holding a short period is indispensable for the densification. Further investigations with more sintering measurement and stricter control grain growth are necessary to optimize the process and improve the properties of the fibers. The experiments show that the grains of sintered ZrO₂ fibers at 1,300 °C up to 1,500 °C (Fig. 10) appear the obvious growth. At this stage, the grain size is sensitive to the holding time, especially at 1,500 °C. When the fiber is held for 5 min, the grain size would increase to ~200 nm, holding for 10 min would result in the formation of ~350 nm particles and apparent pores. Based on the experiments, the suitable sintering temperature is 1,400 °C and time is 30 min, the average size of the grains in ceramics fibers is ~150 nm.

Conclusion

The spinnable zirconium sol was prepared by electrolyzing the mixed solution of ZrOCl₂ · 8H₂O, Y(NO₃)₃ · 6H₂O, sugar and acetic acid. The addition of sugar and CH₃COOH increases the sol stability during the electrolysis, the carboxyl group with Zr(IV) complex produces the linear zirconium acetate polymers, which is responsible for the spinnability. Slow heating the gel fibers before 600 °C is necessary to obtain the dense ZrO₂ fibers. The obvious grain growth appears from 1,300 to 1,500 °C, and the suitable sintering temperature is 1,400 °C, and the average size of the grains in final fibers is ~150 nm.

References

- Garvie RC, Hannink RH, Pascoe RT (1975) *Nature* 258:703
- Yermolenko IN, Vityaz PA, Ulyanova TM (1985) *Sprechsaal* 118:323
- Abe Y, Kudo T, Tomioka H, Gunji T, Nagao Y, Misono T (1998) *J Mater Sci* 33:1863
- Yogo T (1990) *J Mater Sci* 25:2394
- Marshal DB, Lange FL, Morgan PD (1987) *J Am Ceram Soc* 70:187
- De G, Chatter A, Ganguli D (1990) *J Mater Sci Lett* 9:845
- Emig G., Wirth R (1994) *J Mater Sci Lett* 29:4559
- Blaze JE (1967) US Patent 3322865
- Morton MJ, Birchall JD, Cassidy JE (1974) UK Patent 1360199
- Manfred P, Klaus A, Klaus-Dieter F, Wolfhang H, Matthias SM (1995) US Patent 5378400
- He T, Jiao XL, Chen DR (2001) *J Non-Cryst Solids* 283:56
- Zhang LT (1988) *The carbohydrates chemistry*. Light industry Press, Beijing, in Chinese
- Danielson ND, Heenan CA, Haddadian F (1999) *Microchem J* 63:405
- Aelion A, Loebel A, Eirich F (1950) *J Am Chem Soc* 72:5702
- Nakamoto K (1986) *Infrared and Raman spectra of inorganic and coordination compounds*. Wiley-Interscience, New York
- Sakka S, Yoko T (1992) *J Non-Cryst Solids* 147&148:394
- Huggins ML (1942) *J Am Chem Soc* 64:2716
- Einstein A (1906) *Ann Phys* 19:289
- Sakka S, Kozuka H (1988) *J Non-Cryst Solids* 100:142
- Vasko PD, Blackwell J, Koenig JL (1972) *Carbohydrate Res* 23:407
- Korolevich MV, Zhabankov RG, Sivchik VV (1990) *J Mol Struct* 220:301
- Geiculescu AC, Spencer HG (2000) *J Sol-Gel Sci Tech* 17(1):25
- Komissarova LN, Prozorovskaya ZN, Spitsyn VI (1966) *Russ J Inorg Chem* 11(9):2035
- Straughan BP, Moore W, McLaughlin R (1986) *Spectrochim Acta A* 42(4):451
- Zarzycki J, Prassas M, Phalippou J (1982) *J Mater Sci Lett* 17:3371
- Scherer GW (1989) *J on-Cryst Solids* 109:171